A Nonlinear Discrete-time Observer for Inverter Control

N. Léchevin, C.A. Rabbath, S. Lahaie and M. Dostie

Abstract— **A discrete-time high-gain observer is designed in order to estimate the DC voltage of an inverter used as a dynamic electric load emulator. Since the use of LMI techniques makes it possible to obtain a stable observer for a range of bounded duty ratio, the nonlinear-in-the-input average model, which can be expressed as a linear parameter-varying system, is formulated in polytopic form. A robustified version is proposed when exogenous disturbances such as current injection on DC side are present. The nonlinear observers are then discretized, with the hold-equivalent technique, in order to achieve both numerical stability and accuracy as the sampling rate is increased. Nonlinear observer designs proposed in this paper are validated by means of numerical simulations that demonstrate the stability property and performance recovery of a typical state feedback scheme by a high-gain observer-based output feedback.**

I. Introduction

In order to perform a variety of tests of the distributed resources (DR) (fuel cell, microturbines,) without having all the necessary facilities (motors, special nonlinear loads, local power grid, etc), an electric load emulator has been constructed so as to reproduce as faithfully as possible the behavior of a desired electromechanical load. This approach is dual to the programmable dynamometer used to test adjustable speed drives [1]. The control of the inverter aims at tracking the current trajectory provided by a load model whose input signal is the DR voltage. In the past decade, numerous nonlinear controllers have been developed to regulate the current trajectory of similar devices, such as STATCOM, UPFC, and unit power factor rectifier, whose purpose is generally reactive/active power and/or harmonic compensation. See e.g. [2,3] and references therein. These control schemes generally require the measurement of the whole system state. For cost effectiveness, this paper proposes an observer that estimates the DC voltage from the measurement of the DR output voltage and current. The six-pulse power converter average model is bilinear in its input signals (duty ratio). To circumvent the nonlinearities, a polytopic form of the model is derived. A multiobjective LMI design is formulated. This leads to a high-gain observer, which allows recovering the performance of a state feedback control [7]. Under mild assumptions, a hold-equivalent discrete-time (DT) model is derived from the continuous-time (CT) observer. Also DT observer is derived so as to improve exogenous disturbance rejection. Such disturbances arise from current injection on DC side and parasitic uncertainties.

The paper is organized as follows. The average CT model of the inverter is derived in section 2. The LMI-based design of the observer is presented in section 3. Robustness analysis and synthesis of a disturbance attenuation observer are exposed in section 4. The discretization procedure is detailed in section 5. Digital simulations are provided in section 6.

N. Léchevin is with Hydro-Québec Research Chair on Electrical Power and Energy, Université du Québec, Trois-Rivières, QC, Canada G9A 5H7.
C.A. Rabbath is with Defence Research and Development Canada - Valcartier, Val-Belair, QC, Canada G3J 1X5 and with Department of Mechanical Engineering, McGill University, Montréal, QC, Canada H3A 2K6. camille-alain.rabbath@drdc-rddc.gc.ca
S. Lahaie and M. Dostie are with Laboratoire des Technologies de l'Énergie (LTE), Hydro-Québec Research Institute, 600, Avenue de la Montagne, Shawinigan (Québec), Canada G9N 7N5.

II. Continuous -time Model

The system consists of a DR under test (microturbine, fuel cell, etc), and a programmable dynamic electric load whose goal is to emulate an actual load. The emulator is composed of a DSP-controlled inverter. The inverter, which is connected to a rectifier, is essentially composed of six self-commutated IGBTs with anti-parallel diodes, a R_cC passive filter connected to a rectifier (not shown in Fig. 1). The switching frequency is 50 kHz. As a simplified CT model to be used for the observer design, the rectifier block is neglected and will be discussed in the section on robustness issues. From Kirchoff's law (Fig. 1), application of the Blondel-Park transformation, and then from averaging the obtained *abc* dynamics (average state model) whose control signal is compared to a high frequency PWM the following dq system is obtained

$$\begin{bmatrix} \dot{i}_d \\ \dot{i}_q \\ \dot{v}_{dc} \end{bmatrix} = \begin{bmatrix} -\frac{R_f}{L_f} & \omega & 0 \\ -\omega & -\frac{R_f}{L_f} & 0 \\ 0 & 0 & -\frac{1}{R_cC} \end{bmatrix} \begin{bmatrix} i_d \\ i_q \\ v_{dc} \end{bmatrix} + \begin{bmatrix} \frac{v_d}{L_f} \\ \frac{v_q}{L_f} \\ 0 \end{bmatrix} + \begin{bmatrix} -\frac{v_{dc}\rho_d}{L_f} & 0 \\ 0 & -\frac{v_{dc}\rho_q}{L_f} \\ \frac{3i_d\rho_d}{2C} & \frac{3i_q\rho_q}{2C} \end{bmatrix} \quad (1)$$

with $\mathbf{v}_{dq} = \begin{bmatrix} v_d & v_q \end{bmatrix}^T$ and $\mathbf{i}_{dq} = \begin{bmatrix} i_d & i_q \end{bmatrix}^T$ the direct and

quadrature axis components of $\mathbf{v}^s_{abc}$ and $\mathbf{i}_{abc}$; $\rho_{dq} = \left[\rho_d \; \rho_q\right]^T$ the duty ratio that depends on the control inputs representing the modulating signals employed in the PWM. The averaged model given by (4) will be used for control design as a CT invariant model of the converter. It should be noted that this system is nonlinear in the control input, and that an abuse of notation has been made by using $\mathbf{i}_{dq}$ for the averaged signals. In the sequel, it is proposed to estimate the rectified voltage while measuring the source voltage v_{dq} and line current i_{dq}.

III. Continuous -time Observer

The nonlinear system model can be formulated as a linear time-varying system with an input-dependent matrix

$$\begin{bmatrix} \dot{i}_d \\ \dot{i}_q \\ \dot{v}_{dc} \end{bmatrix} = A(\rho_{dq}) \begin{bmatrix} i_d \\ i_q \\ v_{dc} \end{bmatrix} + \frac{1}{L_f} \begin{bmatrix} v_d \\ v_q \\ 0 \end{bmatrix} \tag{2}$$

As input signal ρ_{dq}, state variable i_{dq} and exogenous input v_{dq} are measurable, the following observer

$$\frac{d}{dt} \begin{bmatrix} \hat{i}_d \\ \hat{i}_q \\ \hat{v}_{dc} \end{bmatrix} = A(\rho_{dq}) \begin{bmatrix} \hat{i}_d \\ \hat{i}_q \\ \hat{v}_{dc} \end{bmatrix} + \frac{1}{L_f} \begin{bmatrix} 1 & 0 \\ 0 & 1 \\ 0 & 0 \end{bmatrix} \begin{bmatrix} v_d \\ v_q \end{bmatrix} + K\tilde{i}_{dq} \tag{3}$$

with $\tilde{i}_{dq} = \hat{i}_{dq} - i_{dq}$, gives the following error dynamics

$$\frac{d}{dt} \begin{bmatrix} \tilde{i}_d \\ \tilde{i}_q \\ \tilde{v}_{dc} \end{bmatrix} = \left(A(\rho_{dq}) + KC\right) \begin{bmatrix} \tilde{i}_d \\ \tilde{i}_q \\ \tilde{v}_{dc} \end{bmatrix}$$

where $C = \begin{bmatrix} 1 & 0 & 0 \\ 0 & 1 & 0 \end{bmatrix}$ and $K = \begin{bmatrix} K_{11} & K_{12} \\ K_{21} & K_{22} \\ K_{31} & K_{32} \end{bmatrix}$. The gain matrix K is obtained, via LMIs, such that the eigenvalues of $\left(A(\rho_{dq}) + KC\right)$ have real parts located to the left-hand side of a prescribed negative value. Under the usual operating conditions the duty ratio is bounded as $\left\|\rho_{dq}\right\| \neq 0$. Assume that $\rho_q \neq 0$ and define the bounds $0 \le \underline{\rho_d} \le \rho_d \le \overline{\rho_d}$, $0 \le \underline{\rho_q} \le \rho_q \le \overline{\rho_q}$. The input-dependent matrix A is expressed in the following polytopic form [4]

$$\begin{aligned} A(\rho_{dq}) = {} & \rho_1(\rho_d) A(2\underline{\rho_d}, 2\underline{\rho_q}) + \rho_2(\rho_d) A(2\overline{\rho_d}, 2\underline{\rho_q}) \\ & + \rho_1(\rho_q - \underline{\rho_q}) A(0, 2\underline{\rho_q}) + \rho_2(\rho_q - \underline{\rho_q}) A(0, 2\underline{\rho_q}) \end{aligned} \tag{4}$$

where $\rho_1(x) = \frac{1}{2} \frac{\bar{x} - x}{\bar{x} - \underline{x}}$ and $\rho_2(x) = \frac{1}{2} \frac{x - \underline{x}}{\bar{x} - \underline{x}}$ such that $\sum_{\substack{i=1,2 \\ j=d,q}} \rho_i(\rho_j) = 1$. $\underline{\rho_q} \neq 0$ is considered in order to warrant the observability of the system (A, C). Note that observability is preserved as long as $\underline{\rho_q} \neq 0$ even if $\underline{\rho_d} = 0$. From [5], eigenvalues of $\left(A(\rho_{dq}) + KC\right)$ are located on the left-hand side of h for all ρ_{dq} constrained by (4) if the following LMI

$$PA + A^T P + NC + C^T N^T + 2hP < 0$$

is satisfied at each vertex A of the convex hull $\left(A(2\underline{\rho_d}, 2\underline{\rho_q}), A(2\overline{\rho_d}, 2\underline{\rho_q}), A(0, 2\underline{\rho_q}), A(0, 2\underline{\rho_q})\right)$ and where $N=PK$ and P is a symmetric positive definite matrix.

IV. Robustness issue

A. Robustness analysis

Consider the case where the rectified voltage time constant $\tau_c = R_c C$ is not well-known and is estimated as τ_{co}. Furthermore, suppose that the rectifier shown in Fig. 1 injects a current i_r. Then, system (2) becomes

$$\frac{d}{dt} \begin{bmatrix} i_d \\ i_q \\ v_{dc} \end{bmatrix} = A(\rho_{dq}) \begin{bmatrix} i_d \\ i_q \\ v_{dc} \end{bmatrix} + \frac{1}{L_f} \begin{bmatrix} 1 & 0 \\ 0 & 1 \\ 0 & 0 \end{bmatrix} \begin{bmatrix} v_d \\ v_q \end{bmatrix} + \frac{1}{C} \begin{bmatrix} 0 \\ 0 \\ i_r \end{bmatrix}$$

Using the observer (3) where $A(\rho_{dq})$ is now $\hat{A}(\rho_{dq})$ (i.e. τ_{co} is considered), the estimation error dynamics becomes

$$\frac{d}{dt} \begin{bmatrix} \tilde{i}_d \\ \tilde{i}_q \\ \tilde{v}_{dc} \end{bmatrix} = \left(A(\rho_{dq}) + KC\right) \begin{bmatrix} \tilde{i}_d \\ \tilde{i}_q \\ \tilde{v}_{dc} \end{bmatrix} + \begin{bmatrix} 0 & 0 & \frac{\tau_{co} - \tau_c}{\tau_{co}\tau_c} v_{dc} - \frac{i_r}{C} \end{bmatrix}^T$$

From [7, p. 267], there exists two constants $a_i, b_i > 0$ and $t_0 \in R^+$ such that, for any $t \ge t_0$,

$$\left\| \begin{bmatrix} \tilde{i}_d(t) \\ \tilde{i}_q(t) \\ \tilde{v}_{dc}(t) \end{bmatrix} \right\| = a e^{\lambda_M (t - t_o)} \left\| \begin{bmatrix} \tilde{i}_d(0) \\ \tilde{i}_q(0) \\ \tilde{v}_{dc}(0) \end{bmatrix} \right\| + \frac{a}{\lambda_M b} \left(1 - e^{\lambda_M (t - t_o)}\right) \varepsilon_{v,i} \tag{5}$$

where $\lambda_M = \max\left(\lambda\left(A(\rho_{dq}) + KC\right)\right) < 0$ and $\lambda(.)$ is the eigenvalues of a given matrix and where the following bound is considered $\varepsilon_{v,i} = \max_{v_{dc}, i_r} \left\| \begin{bmatrix} 0 & 0 & \frac{\tau_{co} - \tau_c}{\tau_{co}\tau_c} v_{dc} - \frac{i_r}{C} \end{bmatrix}^T \right\|$

From (5), the steady-state error for $\tilde{i}_{dq}$ and $\tilde{v}_{dc}$ is proportionally bounded to λ_M^{-1}. Therefore, since the system is observable, with a sufficiently high gain (i.e. large $\left|\lambda_M\right|$) used in the observer, although not too high in order to avoid noise amplification, the steady-state error can be made practically acceptable (i.e. 1-2% of nominal value). Although the system is nonlinear, such a high-gain observer (with a saturating function to prevent it from peaking) enables the performance recovery (in the sense of asymptotic stability and trajectories) of usual state-feedback control of the inverter by means of output feedback [7].

B. Robustness synthesis

In order to improve the disturbance rejection property of

the observer, a robust H_∞-based synthesis is performed. Considering observer (3) where $K\tilde{i}$ is replaced by an auxiliary input u_o to be determined, the error dynamics can be rewritten as

$$\frac{d}{dt}\begin{bmatrix}\tilde{i}_d\\ \tilde{i}_q\\ \tilde{v}_{dc}\end{bmatrix} = A\begin{bmatrix}\tilde{i}_d\\ \tilde{i}_q\\ \tilde{v}_{dc}\end{bmatrix} + B_1[d\ \ w] + B_2 u_o;\ z=\begin{bmatrix}\tilde{i}_d & \tilde{i}_q & \tilde{v}_{dc}\end{bmatrix}^T;\ y=\begin{bmatrix}\tilde{i}_d & \tilde{i}_q\end{bmatrix}^T$$

where $w=\Delta z$, $\Delta=\dfrac{\Delta'}{\gamma}$, ($\gamma$ is a normalization factor:

$$\gamma \geq \max_{\rho_d^\delta,\rho_q^\delta}\left\|\Delta'\right\|),\ B_1=\left[\begin{array}{c|c}\gamma I_2 & \begin{matrix}0\\0\end{matrix}\end{array}\right],\ B_2=I_3$$

$$\Delta'=\begin{bmatrix}0 & 0 & -\dfrac{\rho_d^\delta}{L_f}\\ 0 & 0 & -\dfrac{\rho_q^\delta}{L_f}\\ \dfrac{3\rho_d^\delta}{2C} & \dfrac{3\rho_q^\delta}{2C} & 0\end{bmatrix},\ A=\begin{bmatrix}-\dfrac{R_f}{L_f} & \omega & -\dfrac{\rho_d^o}{L_f}\\ -\omega & -\dfrac{R_f}{L_f} & -\dfrac{\rho_q^o}{L_f}\\ \dfrac{3\rho_d^o}{2C} & \dfrac{3\rho_q^o}{2C} & -\dfrac{1}{R_cC}\end{bmatrix},$$

$\rho_{dq}=\rho_{dq}^o+\rho_{dq}^\delta$ ((°) and (δ)) upperscripts correspond to nominal and deviation values *d* represents an exogenous disturbance and u_o is the output of a dynamic systems (6)

$$(U_o)\begin{cases}\dfrac{dz}{dt}=A_o z+B_o y\\ u_o=C_o z+D_o y\end{cases} \tag{6}$$

whose design is conducted by the minimization of the closed-loop L_2 gain between the inputs (*d,w*) and the output *z*. From section 3, operator Δ is bounded and then normalized ($\Delta\in[-1,1]$) so that system (6) is devised in an H_∞- optimal framework. System (U_o) is computed using the Matlab LMI toolbox along with the specification of the following convex pole placement region: (i) Disk with center zero and radius 5000 to prevent from too fast dynamics; (ii) Left-half plane with abscissa –1000 in order to ensure fast convergence of the estimation; (iii) Conic sector with tip abscissa zero and sector angle $\pi/2$ ($\pi/4$ with respect to X-axis). Then, the robust version of observer (3) is formulated as follows

$$\frac{d}{dt}\begin{bmatrix}\hat{i}_d\\ \hat{i}_q\\ \hat{v}_{dc}\\ \hline z\end{bmatrix}=\left[\begin{array}{c|c}A(\rho_{dq})+D_oC_2 & C_o\\ \hline B_oC_2 & A_o\end{array}\right]\begin{bmatrix}\hat{i}_d\\ \hat{i}_q\\ \hat{v}_{dc}\\ \hline z\end{bmatrix}+\frac{1}{L_f}\begin{bmatrix}I_2\\ O_{42}\end{bmatrix}\begin{bmatrix}v_d\\ v_q\end{bmatrix}-\left[\begin{array}{c}D_oC_2\\ \hline B_oC_2\end{array}\right]\begin{bmatrix}i_d\\ i_q\\ \hline v_{dc}\end{bmatrix} \tag{7}$$

where $C_2=\left[\begin{array}{c|c}I_2 & \begin{matrix}0\\0\end{matrix}\end{array}\right]$ and O_{42} is the 4×2 zero matrix.

V. Discrete -time Observer Design

A. Discretization of constant gain observer

Usually mapping techniques are used to discretize the nonlinear observer (3). Trapezoidal mapping, such as the Tustin's method [11], is commonly implemented and gives satisfactory results in terms of numerical stability and accuracy. However, bi-properness of the trapezoidal mapping induces a feedthrough, which has to be avoided in practical digital implementations by inserting an artificial delay at the output of the controller. Hold-equivalent discretization techniques are well suited to system (3) since they avoid the use of a delay while generally preserving the stability and accuracy properties at reasonable sampling rates. The simplest hold-equivalent discretization technique results in a DT system named a step invariant model, where a zero-order hold (ZOH) is placed in front of the CT system and an ideal sampler follows the system [10]. In this paper, hold-equivalent discretization is carried out on the nonlinear-in-the-input (ρ_{dq}) CT observer (3). By noticing that rectified voltage v_{dc} dynamics is much slower than current i_{dq} dynamics, one can reasonably assume that v_{dc} is constant during one time step integration of the i_{dq} dynamics. Therefore, system (3) presents a lower-triangular structure [8] that permits to successively compute the DT i_{dq} and v_{dc} dynamics. i_{dq} dynamics of (3) is rewritten as follows

$$\frac{d\hat{i}_{dq}}{dt}=A_{dq}\hat{i}_{dq}-\frac{\rho_{dq}v_{dc}}{L_f}+w_{dq} \tag{8}$$

with $A_{dq}=\dfrac{1}{L_f}\begin{bmatrix}-R_f & L_f\omega\\ -L_f\omega & -R_f\end{bmatrix}+\begin{bmatrix}K_{11} & K_{12}\\ K_{21} & K_{22}\end{bmatrix}$, $w_{dq}=\dfrac{v_{dq}}{L_f}$ $-\begin{bmatrix}K_{11} & K_{12}\\ K_{21} & K_{22}\end{bmatrix}i_{dq}$. ZOH is used for its simplicity (low-computational complexity) and its satisfactory numerical properties. ZOH applied to (8) leads to

$$\hat{i}_{dq,k+1}=e^{A_{dq}T_s}\hat{i}_{dq,k}+A_{dq}^{-1}\left(e^{A_{dq}T_s}-I_2\right)\left(w_{dq,k}-\frac{\rho_{dq,k}\hat{v}_{dc,k}}{L_f}\right) \tag{9}$$

where subscript k stands for the DT value at $t=kT_s$, $k\in N$ and T_s is the sampling time. Now, the v_{dc} dynamics is expressed as follows

$$\frac{d\hat{v}_{dc}}{dt}=-\frac{\hat{v}_{dc}}{R_cC}+\frac{3\rho_{dq}^T i_{dq}}{2C}+w_{dc}+\begin{bmatrix}K_{31} & K_{32}\end{bmatrix}\hat{i}_{dq}$$

The CT lifted [9] formulation of (7) is expressed as

$$\hat{v}_{dc,k}(\tau)=e^{-\frac{\tau}{R_cC}}\hat{v}_{dc,k}+\int_0^\tau e^{-\frac{\tau-\upsilon_s}{R_cC}}\left(\frac{3\rho_{dq,k}^T(\upsilon)i_{dq,k}(\upsilon)}{2C}+w_{dc,k}(\upsilon)+\begin{bmatrix}K_{31} & K_{32}\end{bmatrix}\hat{i}_{dq,k}(\upsilon)\right)d\upsilon \tag{10}$$

where $\hat{v}_{dc,k}(\tau)=\hat{v}_{dc}(kT_s+\tau)$ for $\tau\in[0,T_s[$. Note that $\hat{v}_{dc,k}(T)=\hat{v}_{dc,k+1}$. The ZOH is applied to the $w_{dc,k}(\upsilon)$ and $\rho_{dq,k}^T(\upsilon)$ input signals. $i_{dq,k}(\upsilon)$ is derived from (9) where T_s is replaced with τ. After substitution of $i_{dq,k}(\upsilon)$ in (10), matrix calculations and replacement of τ by T_s, as a final step, the following DT equation is obtained

$$\hat{v}_{dc,k+1} = e^{-\frac{T_s}{R_c C}}\hat{v}_{dc,k} + R_c C\left(1-e^{-\frac{T_s}{R_c C}}\right)w_{dc,k} + \left(F + R_c C\left(1-e^{-\frac{T_s}{R_c C}}\right)\left(w_{dq,k}^T - \frac{\rho_{dq,k}^T \hat{v}_{dc,k}}{L_f}\right)A_{dq}^{-T}\right)\left(\frac{3}{2C}\rho_{dq,k} + \begin{bmatrix}K_{31}\\K_{32}\end{bmatrix}\right) \quad (11)$$

where $F = \left[\begin{array}{c|c} \hat{i}_{dq,k}^T & w_{dq,k}^T - \dfrac{\rho_{dq,k}^T \hat{v}_{dc,k}}{L_f}\end{array}\right]\left(\dfrac{I_2}{R_c C} + A_{dq}^T\right)^{-1} \times \left(e^{A_{dq}^T T_s} - e^{-\frac{T_s}{R_c C}} I_2\right) I_4 \left[\begin{array}{c} I_2 \\ \hline A_{dq}^{-T}\end{array}\right]$ and I_n is the $n \times n$ identity matrix. The DT observer is composed of (9) and (11).

Remarks: (i) The observer is generally implemented in the same card as the controller and uses the digital quantity $\rho_{dq,k}$ and the sampled signal $i_{dq,k}$ that results from the current measurement of the inverter. Moreover, the inverter constitutes a sampled-data system, i.e. the input signal $\rho_{dq,k}$ is held through a ZOH and the output $i_{dq,k}$ is sampled. A natural way of considering the observer design would be to discretize (2) with the hold-equivalent method presented in this section and then to derive the observer in DT. Mainly two reasons motivate the discretization step of the CT observer: (i) due to the matrix exponential, the discretization hides any physical insight initially associated to the CT model; (ii) DT transition matrix $A(\rho_{dq}, \rho_{dq}^T M \rho_{dq})$ of (2) now depends on quadratic form $\rho_{dq}^T M \rho_{dq}$ which makes the polytopic form derivation more complex to tackle. (ii) Due to the time scale separation between i_{dq} and v_{dc}, a multirate discretization could be performed and implemented as a multirate observer with the help of the DT lifting. Though more accurate, such an approach would lead to an observer whose complexity increase is a function of the ratio of the different sample time used for i_{dq} and v_{dc}.

B. Discretization of dynamic gain observer

The observer (7) is not in lower-triangular form and a new scheme for discretization should be applied. Lower triangularization of (7) is too complex mainly because of the time-varying nature of $A(\rho_{dq})$. Note that bilinearities only involve multiplication of state variables with input signals. Integration of (7) is then possible and leads to

$$\begin{bmatrix}\hat{i}_{d,k+1}\\ \hat{i}_{q,k+1}\\ \hat{v}_{dc,k+1}\\ \hline z_{k+1}\end{bmatrix} = \phi_k(0,T_s)\begin{bmatrix}\hat{i}_{d,k}\\ \hat{i}_{q,k}\\ \hat{v}_{dc,k}\\ \hline z_k\end{bmatrix} + \int_0^{T_s}\phi_k(\tau,T_s)p(\tau)d\tau \quad (12)$$

where $p = \dfrac{1}{L_f}\begin{bmatrix}I_2\\ O_{42}\end{bmatrix}\begin{bmatrix}v_d\\ v_q\end{bmatrix} - \left[\begin{array}{c}D_o C_2\\ \hline B_o C_2\end{array}\right]\begin{bmatrix}i_d\\ i_q\\ v_{dc}\end{bmatrix}$ and $\phi_k(0,T_s)$ is the transition matrix associated to $\mathcal{A}(\rho_{dq}) = \left[\begin{array}{c|c}A(\rho_{dq}) + D_o C_2 & C_o\\ \hline B_o C_2 & A_o\end{array}\right]$. To compute (12), hold devices are now used to approximate input signals located at two different places, i.e. the actual plant input ρ_{dq} in $\phi_k(0,T_s)$ (i.e. in $\mathcal{A}$) and the observer input p. For each entry a specific hold (H_ρ, H_p) could be used in order to take into account each input's own behavior (time scale separation, causality constraint, continuity property). To constrain computational complexity, zero-order holds are considered which means that the input is supposed to be constant during one time step. Therefore, the transition matrix and its integration are computed as follows

$$\begin{aligned}\phi_k(0,T_s) &= \int_0^{T_s}\mathcal{A}(\rho_{dq}(\sigma))d\sigma = \int_0^{T_s}\mathcal{A}(H_\rho(\sigma)\rho_{dq,k})d\sigma \\ &= \mathcal{A}(\rho_{dq,k})T_s \\ \int_0^{T_s}\phi_k(\tau,T_s)p(\tau)d\tau &= \int_0^{T_s} e^{\mathcal{A}(\rho_{dq,k})(T_s-\tau)}H_p(\tau)d\tau \cdot p_k \\ &= \int_0^{T_s} e^{\mathcal{A}(\rho_{dq,k})(T_s-\tau)}d\tau \cdot p_k\end{aligned}$$

Then (12) becomes

$$\begin{bmatrix}\hat{i}_{d,k+1}\\ \hat{i}_{q,k+1}\\ \hat{v}_{dc,k+1}\\ \hline z_{k+1}\end{bmatrix} = e^{\mathcal{A}(\rho_{dq,k})T_s}\begin{bmatrix}\hat{i}_{d,k}\\ \hat{i}_{q,k}\\ \hat{v}_{dc,k}\\ \hline z_k\end{bmatrix} + \mathcal{A}^{-1}(\rho_{dq,k})\left(e^{\mathcal{A}(\rho_{dq,k})T_s} - I_6\right)p_k \quad (13)$$

The time-varying matrix exponential $e^{\mathcal{A}(\rho_{dq,k})T_s} \in \Re^{6\times 6}$ is implemented with Padé approximant (1,2) order so as to meet both requirements of complexity and stability. This choice leads to L-stability numerical property rather than A-stability in the case of Trapezoidal approximation and then is more adequate for system with large eigenvalues.

VI. DIGITAL SIMULATIONS

A. Open-loop validation of the observer

In order to validate the observer design, the average model along with the DT observer is digitally simulated with the following parameters: R_f=1.44Ω, L_f=4.2mH, C=10mF, R_c=80Ω, f=60Hz, $V_{L\text{-}N}$=120V, $\rho_{abc}(t)$=0.1v or 0.9v for t≤0.5 or t>0.5, resp.; $v = [\sin(wt)\ \ \sin(wt-2pi/3)\ \ \sin(wt+2pi/3)]$. Initial estimation errors of $\tilde{i}_{dq}^T = [5\ \ 10]A$ and $\tilde{v}_{dc} = 80V$ are introduced in order to excite the observer dynamics. As future experiments will involve a PWM switching frequency of 50kHz, a sample time T_s of 100µs is used . In order to adequately track the behaviour of load model (induction motor) one wants to emulate a load whose controller is designed to obtain tracking error dynamic time constant of a few ms. As the observer is usually 5 to 10 times faster than the controller, time constants of 500µs are

targeted by imposing $h = 1000$ in (10). Estimated quantities along with their error with respect to the averaged inverter simulated in variable-step mode are displayed in Fig. 2 and 3. Estimated and actual quantities are superimposed and are shown to be very close to each other, which is the reason why the error are displayed. Fig. 4 displays the quadratic error for $T_s \in [0.1,1.5]$ms of the proposed DT observer and a version of the CT observer where integrator $1/s$ is replaced by Tustin's mapping. Each result is compared to the actual averaged inverter simulated with a variable-step size integration method of Simulink. Mention that Euler mapping has been tested and becomes unstable for $T_s > 750\mu s$. Results of hold-equivalent method-based observer compares advantageously to the Trapezoidal ones.

B. Validation of an observer-based control system.

The previous DT observer is used to estimate the DC voltage needed to compute the following DT control law (14) which is based on (i) a dynamic inverse-based feedforward loop and on (ii) a proportional integral feedback loop where the integration numerical approximation is achieved with the Trapezoidal operator.

$$\begin{aligned} \rho_{dq,k} &= \rho^{ff}_{dq,k} + \rho^{fb}_{dq,k}; \\ \rho^{ff}_{dq,k} &= \frac{L_f}{\hat{v}_{dc,k}}\left(A_2 i^*_{dq,k} - A_2^o \tilde{i}_{dq,k} + \frac{v_{dq,k}}{L_f} \right) \\ \rho^{fb}_{dq,k} &= -\frac{L_f}{\hat{v}_{dc}} K_{fb}\left[I_2 \quad \frac{T_s}{2}\frac{z+1}{z-1} \right]^T \tilde{i}_{dq,k} \end{aligned} \tag{14}$$

where A_2 is the 2×2 left upper block of A, i^*_{dq} the desired current trajectory, $A_2^o = \begin{bmatrix} 0 & -\omega \\ \omega & 0 \end{bmatrix}$ and $\hat{v}_{dc}$ the estimated DC voltage computed by the observer (13). The commanded current is computed by the load model one wishes to emulate. The DC voltage is stabilized by the rectifier around 80V. At t=0s , $i^*_{dq} = [1 \;\; 1]^T$ and remains constant until t=0.1s where a step is applied such that $i^*_{dq} = [10 \;\; 0]^T$. A sampling time of $T_s = 100\mu s$ is used. The RC filter of Fig.1 is in fact connected to a rectifier that injects some DC current (around 3.5A) in order to maintain a stabilized DC voltage around a fix value. This current acts like an exogenous disturbance to the observer whose disturbance attenuation property is such that a steady-state estimation error of 0.4V appears (Fig. 6). The impact on the current time responses is negligible (Fig. 5) since they are well superimposed with those resulting from the state feedback controller. No substantial transient deterioration with respect to the state feedback case can be noticed.

REFERENCES

[1] Z. H. Akpolat, G. M. Asher, and J. C. Clare, "Experimental dynamometer emulation of nonlinear mechanical loads," *IEEE Transactions on Industry Applications*, Vol. 35, Iss. 6 , pp. 1367–1373, Nov.-Dec. 1999

[2] G. Escobar, D. Chevreau, R. Ortega and E. Mendes, "An adaptive passivity-based controller for a unity power factor rectifier," *IEEE Transactions on Control Systems Technology*, Vol. 9, Iss. 4 , pp. 637–644, July 2001.

[3] D. Karagiannis, E. Mendes, R. Ortega and A. Astolfi, "Nonlinear control of power factor precompensators: an experimental study," in *Proceedings of the 2002 International Conference on Control Applications*, Vol. 2 , pp. 1252 –1257, 18-20 Sept. 2002

[4] H. Kajiwara, P. Apkarian, P. Gahinet, "LPV techniques for control of an inverted pendulum," *IEEE Control Systems Magazine*, Vol. 19. No. 1 , pp. 44-54, Feb. 1999.

[5] M. Chilali, P. Gahinet, "H_∞ design with pole placement constraints: an LMI approach," *IEEE Transactions on Automatic Control*, Vol. 41, Vol. 3, pp.358-367, March 1996

[6] H. K. Khalil, *Nonlinear Systems*, Prentice Hall, 2nd Edition, 1996.

[7] A. N. Atassi, H. K. Khalil, "A separation principle for the stabilization of a class of nonlinear systems," *IEEE Transactions on Automatic Control*, Vol. 44, No. 9, pp. 1672-1687, Sept. 1999.

[8] P. Albertos, "Sampled-data Modeling and Control of Nonlinear Systems," in *Proceedings of the 35th IEEE Decision and Control*, 11-13 Dec 1996, Vol. 1, pp. 925 –930.

[9] B. Bamieh and J. B. Pearson, "A general framework for linear periodic systems with applications to H_∞ sampled-data control," *IEEE Trans. Automat. Contr.*, vol. 37, pp. 418–435, Apr. 1992.

[10] K. J. Åström and B. Wittenmark, *Computer-Controlled Systems - Theory and Design*, Prentice Hall, Englewood Cliffs, NJ, Second edition, 1990

[11] T. T. Hartley, G. O. Beatle and S. P. Chicatelli, *Digital Simulation of Dynamic Systems - A Control Theory Approach*, Prentice Hall, 1994.

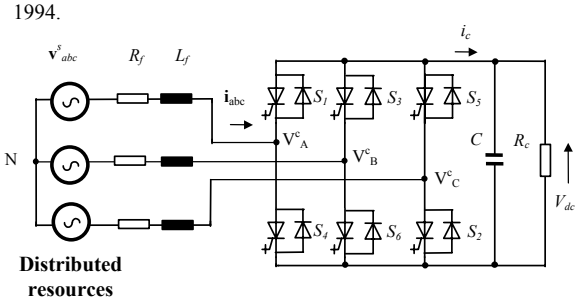

Fig. 1: Power circuit

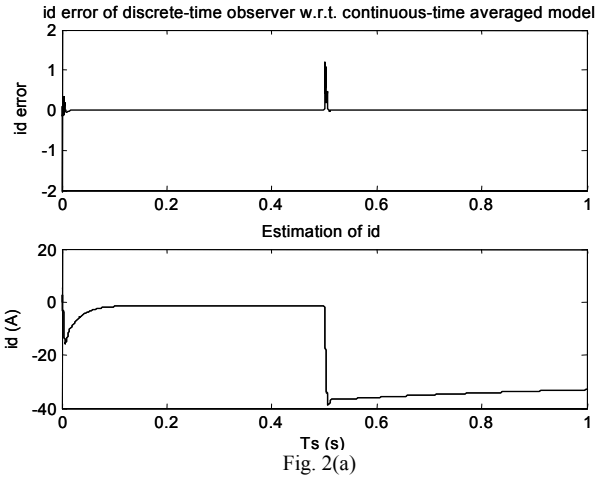

Fig. 2(a)

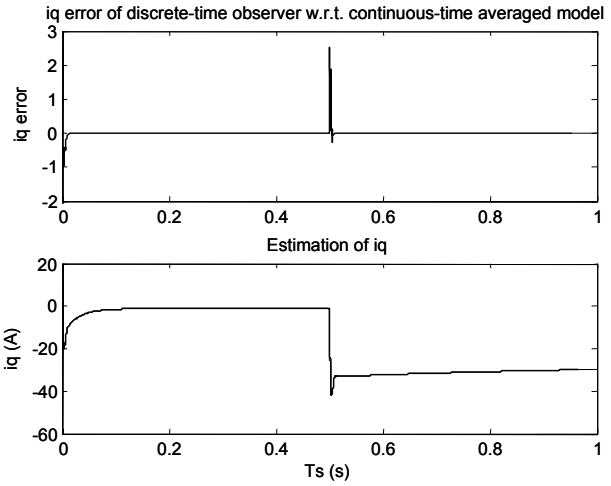

(b)

Fig. 2: Estimated current resulting from the DT observer – comparison with the CT averaged model of the inverter (T_s=100μs); (a) i_d;(b) i_q

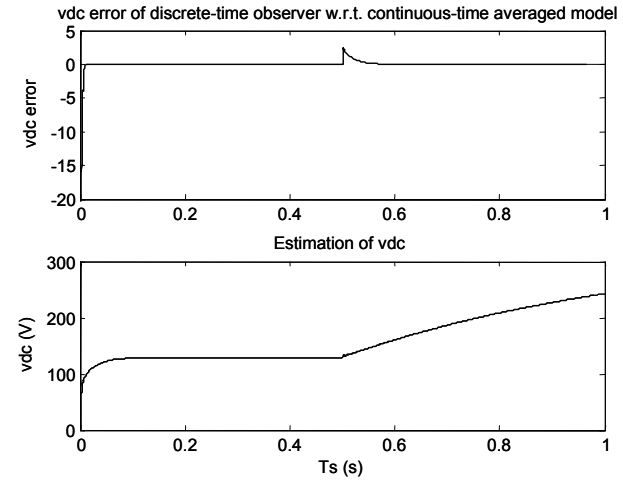

Fig. 3: Estimated rectified voltage (v_{dc}) resulting from the DT observer – comparison with the CT averaged model of the inverter – T_s=100μs

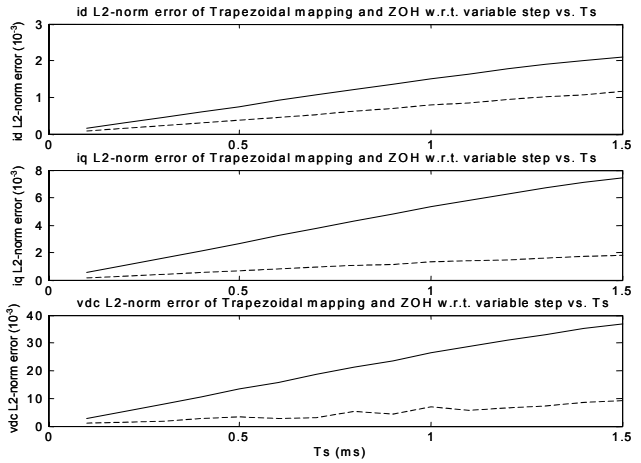

Fig. 4: Comparison of L_2-errors for various DT observers; (-) Trapezoidal mapping, (--) ZOH

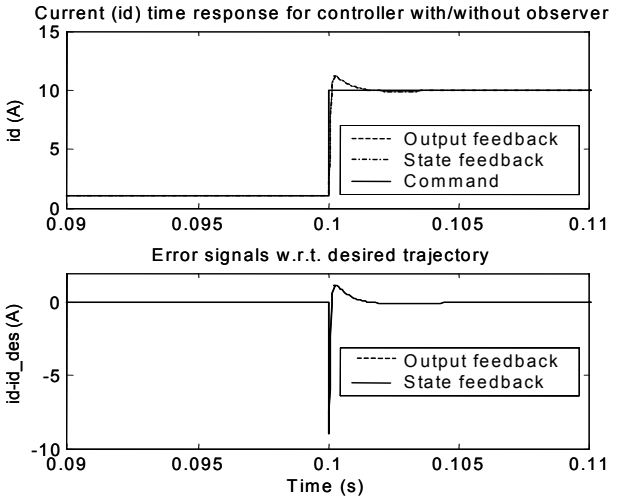

(a)

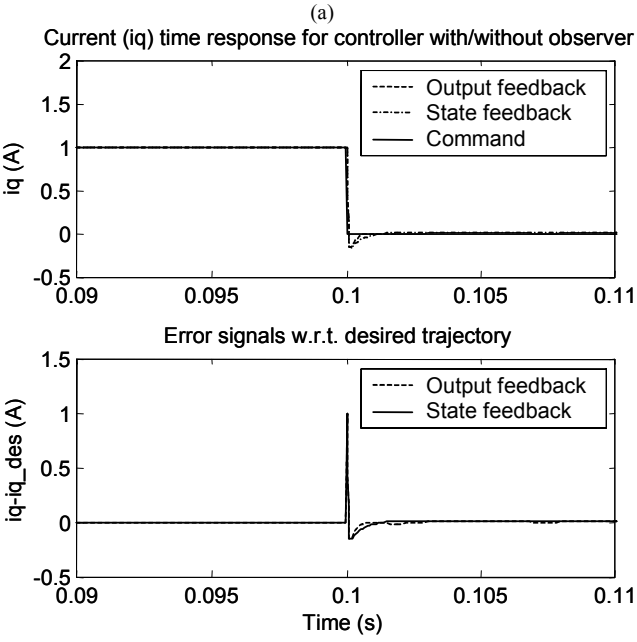

(b)

Fig. 5: Comparison of current time response of the inverter with observer-based controller (--) and state feedback controller (-.); (a) i_d;(b) i_q

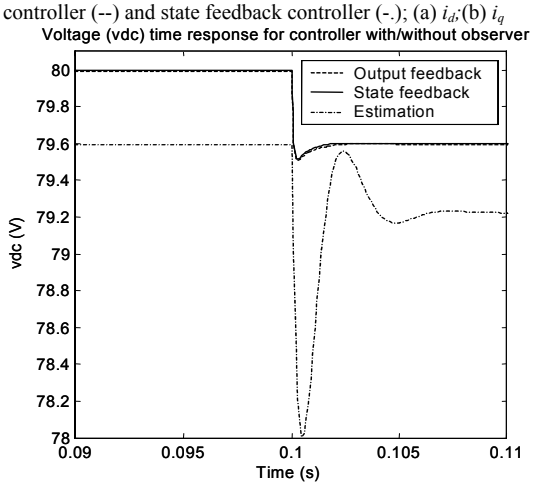

Fig. 6: Comparison of the estimated voltage (-.-) with voltage (v_{dc}) time response of the inverter equipped with observer-based controller (--) and state feedback controller (-)